Parametric instability of an integrated micromechanical oscillator by means of active optomechanical feedback

J. Roels, B. Maes, W. Bogaerts, R. Baets, and D. Van Thourhout*

Photonics Research Group, Department of Information Technology, Ghent University-IMEC Sint-Pietersnieuwstraat 41, B-9000 Gent

**dries.vanthourhout@intec.ugent.be*

Abstract: Mass sensing and time keeping applications require high frequency integrated micromechanical oscillators. To overcome the increasing mechanical stiffness of these structures sensitive optical vibration detection and efficient actuation is required. Therefore we have implemented an active feedback system, where the feedback signal is provided by the optical gradient force that is present between nanophotonic waveguides on a silicon-on-insulator chip. We found that access to the parametric instability regime can be easily controlled by tuning the wavelength.

OCIS codes: (120.4880) Optomechanics; (130.3120) Integrated optics devices.

References and links

1. T. J. Kippenberg and K. J. Vahala, "Cavity optomechanics: back-action at the mesoscale," Science **321**, 1172–1176 (2008).
2. D. Kleckner and D. Bouwmeester, "Sub-kelvin optical cooling of a micromechanical resonator," Nature **444**, 75–78 (2006).
3. A. D. O'Connell, M. Hofheinz, M. Ansmann, R. C. Bialczak, M. Lenander, E. Lucero, M. Neeley, D. Sank, H. Wang, M. Weides, J. Wenner, J. M. Martinis, and A. N. Cleland, "Quantum ground state and single-phonon control of a mechanical resonator," Nature **464**, 697–703 (2010).
4. M. Hossein and K. J. Vahala, "An optomechanical oscillator on a silicon chip," IEEE J. Sel. Top. Quantum Electron. **16**(1), 276–287 (2010).
5. A. Vidic, D. Then, and C. Ziegler, "A new cantilever system for gas and liquid sensing," Ultramicroscopy **97**, 407–416 (2003).
6. J. Tamayo, A. D. L. Humphris, A. M. Malloy, and M. J. Miles, "Chemical sensors and biosensors in liquid environment based on microcantilevers with amplified quality factor," Ultramicroscopy **86**, 167–173 (2001).
7. D. Van Thourhout and J. Roels, "Optomechanical device actuation through the optical gradient force," Nat. Photonics **4**(4), 211–217 (2010).
8. M. Li, W. H. P. Pernice, C. Xiong, T. Baehr-Jones, M. Hochberg, and H. X. Tang, "Harnessing optical forces in integrated photonic circuits," Nature **456**, 480–484 (2008).
9. J. Roels, I. De Vlaminck, L. Lagae, B. Maes, D. Van Thourhout, and R. Baets, "Tunable optical forces between nanophotonic waveguides," Nat. Nanotechnol. **4**(8), 510–513 (2009).
10. M. Li, W. H. P. Pernice, and H. X. Tang, "Tunable bipolar optical interactions between guided lightwaves," Nat. Photonics **3**(8), 464–468 (2009).
11. M. L. Povinelli, M. Loncar, M. Ibanescu, E. J. Smythe, J. Erich, S. G. Johnson, F. Capasso, and J. D. Joannopoulos, "Evanescent-wave bonding between optical waveguides," Opt. Lett. **30**, 3042–3044 (2005).
12. A. Mizrahi and L. Schachter, "Mirror manipulation by attractive and repulsive forces of guided waves," Opt. Express **13**, 9804–9811 (2005).
13. S. K. Selvaraja, P. Jaenen, W. Bogaerts, D. Van Thourhout, P. Dumon, and R. Baets, "Fabrication of photonic wire and crystal circuits in silicon-on-insulator using 193-nm optical lithography," J. Lightwave Technol. **27**(18), 4076–4083 (2009).
14. D. Taillaert, P. Bienstman, and R. Baets, "Compact efficient broadband grating coupler for silicon-on-insulator waveguides," Opt. Lett. **29**, 2749–2751 (2004).

#142630 - $15.00 USD Received 15 Feb 2011; revised 10 Apr 2011; accepted 29 Apr 2011; published 22 Jun 2011

15. R. Kubo, "The fluctuation dissipation theorem," Rep. Prog. Phys. **29**, 255–284 (1966).
16. I. De Vlaminck, J. Roels, D. Taillaert, D. Van Thourhout, R. Baets, L. Lagae, and G. Borghs, "Detection of nanomechanical motion by evanescent light wave coupling," Appl. Phys. Lett. **90**, 233116 (2007).
17. H. Nyquist, "Thermal agitation of electric charge in conductors," Phys. Rev. **32**(1), 110–113 (1928).
18. G. P. Agrawal, *Fiber Optic Communication System* (Wiley, 2002), Chap. 6.
19. E. Säckinger, *Broadband Circuits for Optical Fiber Communication* (Wiley, 2005), Chap. 3.

1. Introduction

Optical cooling of micromechanical resonators has recently attracted a lot of attention in the scientific community [1, 2]. In general the major incentive is the possibility to cool a micromechanical resonator to its quantummechanical ground state [3]. In the case of optical cooling light is used to extract energy from the mechanical resonator and hence to dampen its motion. However it is also possible to reverse this process and amplify the resonator's motion through positive optical feedback. In this regime the micromechanical resonator can be used as an integrated photonic clock [4] or reference oscillator. When thinking of mass sensing applications, especially in a fluidic environment, micromechanical resonators suffer from very low quality factors. This limitation might be overcome by positive feedback [5, 6]. Both for the sensing and reference oscillator applications shifting the oscillator's operating frequency closer to the GHz regime is beneficial.

Passive cooling or amplification requires the mechanical oscillator to be implemented in an optical cavity with high Q because the mechanical oscillation period needs to be on the same order of magnitude as the optical cavity lifetime. However a very high Q limits the intrinsic optical bandwidth of the system. In addition the high circulating optical powers might result in heating of the cavity material. Consequently instability of the optical resonance wavelength can be expected through the thermo-optic effect, which is a considerable drawback.

In this paper we present a system with active feedback that does not include an optical cavity, hence strongly reducing bandwidth and heating issues. The feedback force is the optical force that exists between two nanophotonic integrated waveguides. This type of force has recently been intensively exploited [7, 8, 10]. In an active feedback system the motion of the mechanical resonator is continuously monitored. Using the recorded signal a feedback force that has a distinct phase relation to the oscillator's vibration is generated. If we assume the mechanical oscillator to be harmonic (with spring constant k, effective mass m and damping constant Γ) and a brownian force F_{brown} acting on it, then the system can be modeled as:

$$kx(t) + \Gamma\dot{x}(t) + m\ddot{x}(t) = F_{brown}(t) + F_{fb,opt}(t) \tag{1}$$

The optical feedback force $F_{fb,opt}(t)$ can be thought of as providing an additional damping term $\Gamma_{opt}\dot{x}(t)$ which can be added to the intrinsic damping term at the left hand side of Eq. (1).

The exact phase relation between the oscillating beam and the feedback force of depends on the delay in the feedback loop. However the mechanical oscillation frequencies that we encounter in our optomechanical devices are typically in the range of 2-10 MHz, so tunable delays on the order of a few hundreds of nanoseconds are required to actively control the phase of the feedback force. It is not straightforward to achieve such wide tuning in the delay loop. As an alternative we propose an optomechanical device (shown in Fig. 1(a)) which exhibits an optical force of which the phase can be selected with wavelength. The device consists of a Mach-Zehnder interferometer in which one of the arms is considerably longer than the other. One of the couplers/splitters consists of a freestanding parallel waveguide pair. Due to the different arm lengths the fields arrive with different phases at the entrance of the parallel waveguide section when tuning the pump laser wavelength. The fields arriving in phase will favor the excitation of the symmetric guided mode in the parallel waveguide section, while fields in anti-phase favor

#142630 - $15.00 USD Received 15 Feb 2011; revised 10 Apr 2011; accepted 29 Apr 2011; published 22 Jun 2011

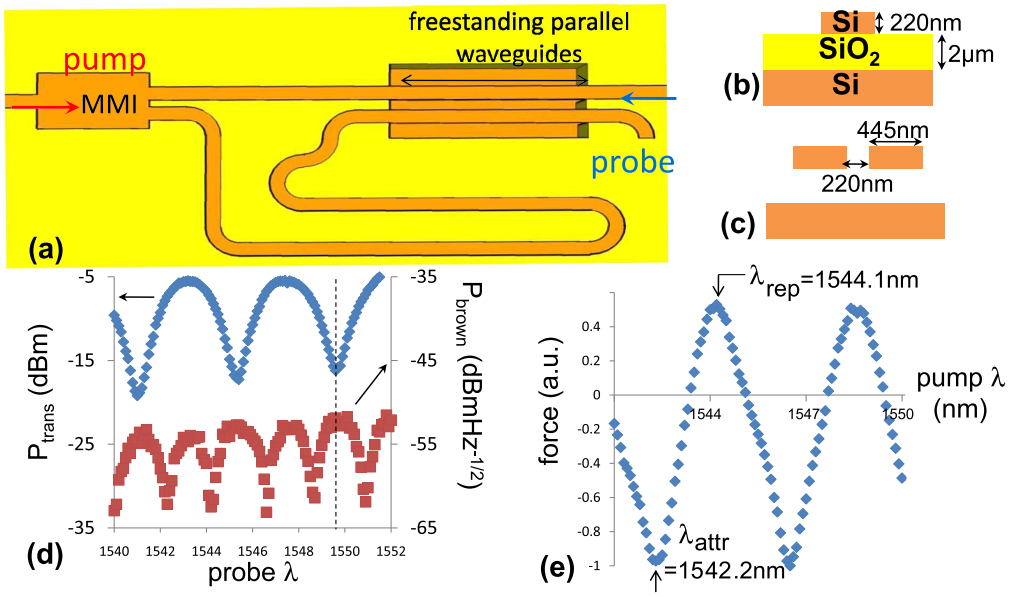

Fig. 1. Tunable force device [9]. (a), Mach-Zehnder interferometer with arms of unequal length, one coupler is a Multi-Mode interferometer (MMI) 3dB-splitter/combiner, the other is a freestanding parallel waveguide coupler. It is also shown where the pump and probe laser light enter the device. (b), Cross-section of a nanophotonic wire in silicon-on-insulator. (c), Cross-section of the freestanding parallel waveguides. (d), Transmission spectrum of the MZI with freestanding waveguide coupler. Also the transduction spectrum (taken by measuring the brownian mechanical response at different probe wavelengths and no pump signal) is plotted, showing that maximum optomechanical transduction can be found at the local maxima and minima of the transmission spectrum. (e), Measured force when sweeping the pump length. For the feedback experiments we use for the pump settings the purely attractive force (1542.2 nm) or the repulsive force (1544.1 nm), and set the probe wavelength to 1549.5 nm (dashed line in (d))

the anti-symmetric mode. The latter corresponds to a repulsive force, the former to an attractive force [11, 12] (Fig. 1(e)). Hence effective phase tuning of the force over the full range of 2π can be achieved. We have fabricated a number of such devices using a silicon-on-insulator platform [13]. The cross-section of the nanophotonic silicon wires is 445 nm width to 220 nm height and the gap between the parallel waveguides is 220 nm (Fig. 1(b) and Fig. 1(c)). Light is coupled into the nanophotonic waveguide using a grating coupler [14]. Typical lengths of the freestanding part vary from 20 to 35 μm.

2. Optimizing motion detection

To initiate the envisioned strongly coherent oscillation a sufficiently strong initial vibration is required to provide the feedback loop with an input signal. The required initial vibration is provided by the thermal brownian force [15]. However since this force is very weak and the optomechanical transduction in the proposed type of device is not extremely high the initiating signal that was obtained in previous work [9, 16] is too weak and noisy. Consequently we first carefully analyze the noise factors that limit the transduction and optimize our detection scheme.

In our setup the motion is registered through a probe signal that passes through the op-

#142630 - $15.00 USD Received 15 Feb 2011; revised 10 Apr 2011; accepted 29 Apr 2011; published 22 Jun 2011

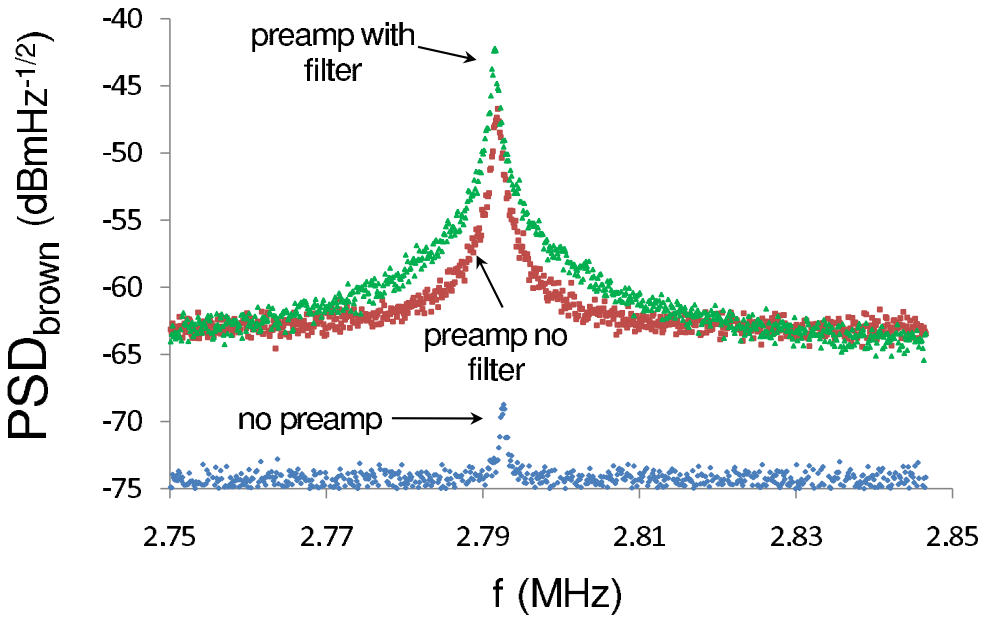

Fig. 2. The blue trace (labeled 'no preamp') is the recorded thermal vibration power spectral density (PSD) without optical preamplifier. The noise floor is set by Johnson-Nyquist noise in the optical detector. The red trace (labeled 'preamp, no filter') was obtained by preamplifying the signal with an EDFA. The noise floor is set by spontaneous-spontaneous beat noise. The green trace (labeled 'preamp with filter') was obtained by inserting a 2.4 nm optical bandpass filter after the EDFA. The noise floor is set by signal-spontaneous beat noise. The EDFA and filter provide a 16 dB improvement of the displacement sensitivity.

tomechanical device (approximately 0 dBm through the device). Whenever one of the parallel nanophotonic waveguides is moving, the gap (and the coupling between the waveguides) is altered and by consequence the power splitting ratio of the coupler is also affected [16]. Hence the vibration of the nanophotonic waveguide is imprinted onto the probe signal as a power modulated RF signal and is converted into an electrical RF signal in the photoreceiver. As can be seen in Fig. 1(d) both the transduction and transmission are wavelength dependent. We also note that the optomechanical transduction is most sensitive for wavelengths that correspond to maxima or minima in the transmission spectrum. We choose to set the probe wavelength to a wavelength that corresponds to a minimum in the transmission spectrum. We will comment on this choice when analyzing the limiting noise factors.

The blue trace (labeled 'no preamp') in Fig. 2 was recorded at a local transmission minimum (and hence at a local transduction maximum) of only -37 dBm CW output power (MZI extinction ratio $> 30\,dB$). Please note that the data in Fig. 2 stem from a different device than the data displayed in Fig. 1, Fig. 4, Fig. 5, and Fig. 6, which all origin from the same device for which the suspended waveguides have natural mechanical frequencies 5.98 MHz and 6.239 MHz. We see that the recorded power spectral density (PSD) exceeds the noise floor of the electrical spectrum analyzer (ESA) by only $5\,dB$ approximately at the maximum. The noise floor (and hence the displacement sensitivity) is set by Johnson-Nyquist photoreceiver noise (noise equivalent power photoreceiver = 65 dBm $Hz^{-\frac{1}{2}}$) [17]. This statement is supported by the observation that the same noise floor is measured with and without light being incident on the photoreceiver,

#142630 - $15.00 USD Received 15 Feb 2011; revised 10 Apr 2011; accepted 29 Apr 2011; published 22 Jun 2011

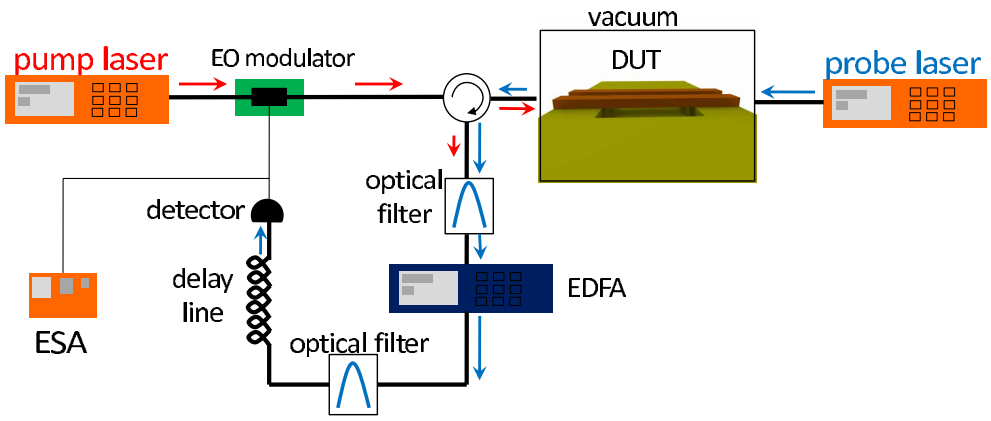

Fig. 3. Experimental pump-probe set-up with feedback loop and enhanced detection scheme. The devices are placed in a vacuum chamber to reduce air damping.

indicating that the laser noise (laser linewidth¡200kHz) is negligible compared to the receiver noise.

In fact a similar noise limitation is encountered in telecom optical networks. When the noise at the receiver side is found to be the dominant noise factor one benefits from preamplifying the optical signal using an optical amplifier [18]. However during the amplification process additional noise is added to the signal. Because the photodetector responds to the intensity, which is proportional to the square of the fields, the optical noise gets converted in two electrical beat noise components. Roughly speaking we get the terms corresponding to $(signal + noise)^2 = signal^2 + noise^2 + 2\,noise\,signal$. The first term is the useful signal, the second term is the spontaneous-spontaneous beat noise and the third term is called the signal-spontaneous beat noise. A more detailed analysis shows that the variance of current fluctuations $\sigma^2 = <(\Delta I)^2>$ due to spontaneous-spontaneous and signal-spontaneous beat noise can be written as [19]:

$$\sigma^2 = \sigma^2_{sig-sp} + \sigma^2_{sp-sp}\sigma^2_{sig-sp} = 4R^2 S_{sp}\Delta f_{elec}\, GP_s\sigma^2_{sp-sp} = 4R^2 S_{sp}\Delta f_{elec}\, S_{sp}\Delta\nu_{opt} \qquad (2)$$

In these formulas P_s is the (DC) optical signal power before amplification, G is the amplifier gain and R is the responsivity of the detector so a signal current $I = RGP_s$ is generated. The spectral density of the spontaneous emission induced noise S_{sp} can also be expressed in terms of the amplifier noise figure F_n, the amplifier gain and the average photon energy $h\nu$: $S_{sp} \approx \frac{1}{2}Gh\nu F_n$. Given the linear and quadratic dependence on F_n of σ^2_{sig-sp} and σ^2_{sp-sp} the importance of an amplifier with low noise figure (the optical amplifiers used in this work have a noise figure of approximately 4.5 dB) is clear. Also the electrical bandwidth Δf_{elec} is of crucial importance, however, reducing the electrical measurement bandwidth is at some point no longer beneficial when characterizing thermal mechanical noise, because both the mechanical and Johnson-Nyquist noise scale with electrical bandwidth.

Due to its dependence on the optical bandwidth $\Delta\nu_{opt}$ the spontaneous-spontaneous beat noise (see Eq. (2)) can in principle easily be reduced by placing an optical band-pass filter after the optical amplifier. So we conclude that ultimately the signal-spontaneous beat noise must limit the achievable displacement sensitivity. Given the dependence of the signal-spontaneous beat noise on P_s we also understand now why it is beneficial to choose a probe wavelength with low intrinsic transmission: the signal-spontaneous noise is reduced to its absolute minimum.

When the optical probe signal is amplified through an EDFA prior to detection ($0\,dBm$ at the

#142630 - $15.00 USD Received 15 Feb 2011; revised 10 Apr 2011; accepted 29 Apr 2011; published 22 Jun 2011

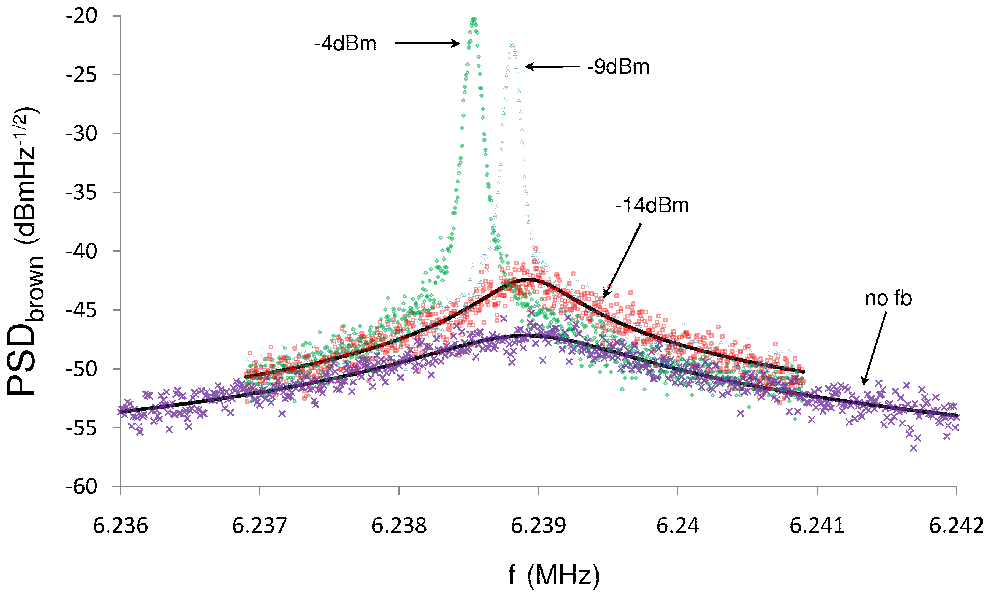

Fig. 4. Feedback experiments for different optical pump powers (estimated power inside the device). The lowest (purple) trace (labeled 'no fb') origins from the thermal brownian vibration without any optical feedback force. When inserting $-14\,dBm$ in the device, then the damping is more than halved and the apparent mechanical Q increases from 4760 to 10300 (values obtained through fits to a Lorentzian model). For higher optical feedback powers we observe strong, coherent oscillations. The measured responses are not Lorentzian for they are strongly influenced by the Gaussian filter shape of the electrical spectrum analyzer. The black solid lines are fits to a Lorentzian model that allows extraction of the Q's.

detector) we obtain the red data points (labeled 'preamp, no filter' in Fig. 2). We see that the noise floor is raised over $11\,dB$, however the useful signal now peaks $16\,dB$ above the noise floor. Knowing that spontaneous-spontaneous beat noise is reduced by reducing the optical bandwidth (but signal-spontaneous noise is not, see Eq. (2)) we placed an optical bandpass filter ($2.4\,nm$ optical bandwidth) after the EDFA and obtained the green data (labeled 'preamp with filter' in Fig. 2). We see that the use of the filter provides us with an additional $5\,dB$ of useful signal and finally we obtain a signal that exceeds the noise floor by $21\,dB$. Additional experiments with smaller bandwidth optical filters ($0.6\,nm$) did not yield any significant improvement, indicating that signal-spontaneous beat noise is the limiting noise factor for the green data series. Compared to the non preamplified trace the overall improvement of the displacement sensitivity ($16\,dB$) is dramatic. After calibration we find that the displacement sensitivity has been improved from approximately 80 to 2 $fmHz^{-\frac{1}{2}}$.

3. Feedback

The obtained electrical signal (improved through optical preamplification) is then used to drive an electro-optical modulator, which modulates the pump laser. The generated optical force that acts onto the optomechanical device closes the feedback loop. The setup is shown in Fig. 3.

In order to access the region with strongly amplified motion the gain in the feedback loop needs to be sufficiently high and the phase of the force needs to be set properly (see Eq. (1)). The gain can be controlled through the optical power that is injected by the pump laser, the phase

#142630 - $15.00 USD Received 15 Feb 2011; revised 10 Apr 2011; accepted 29 Apr 2011; published 22 Jun 2011

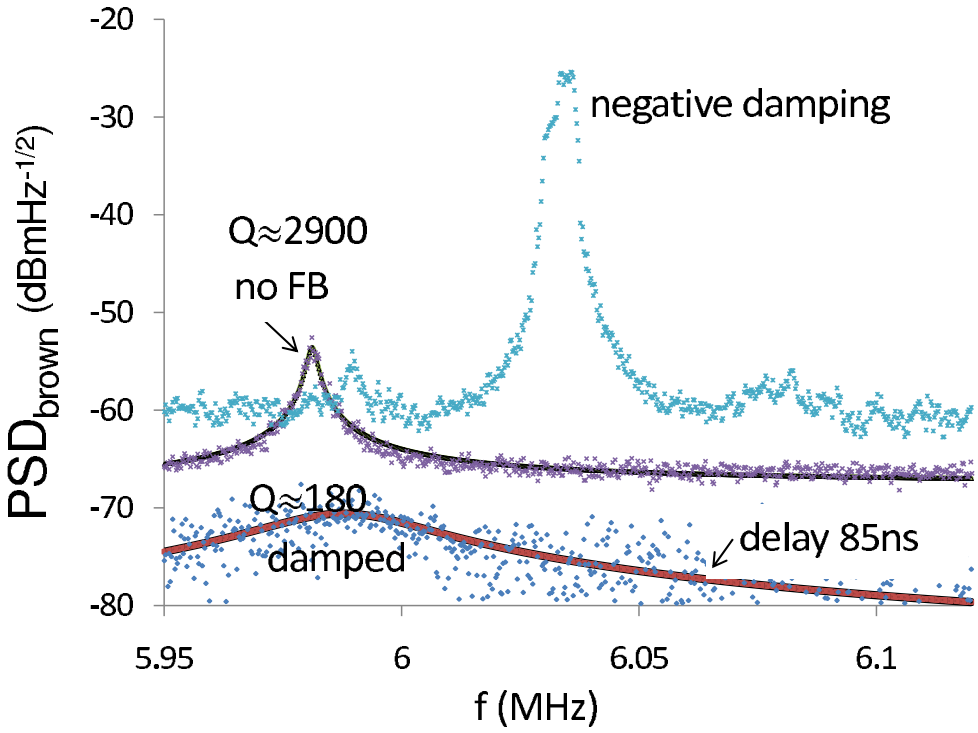

Fig. 5. Feedback experiments for different delay lengths in the feedback loop. The length of the feedback loop was set to achieve maximum damping for λ_{attr}=1542.2 nm (Q≈180, curve labeled '85 ns delay'). The damping increased with a factor of 16 compared to the case without feedback (initial Q=2900). Shortening the feedback loop with 85 ns retrieved strongly amplified motion (curve labeled 'negative damping').

can be controlled by either the length of the feedback loop or the chosen pump wavelength. In order to analyze the influence of the different parameters we will each time vary one parameter (pump power, delay length or wavelength) and keep the two others constant.

In first instance we have established a purely attractive optical force (λ_{attr}=1552.4 nm) and fixed the feedback loop's delay length such that the optical force provides a maximum amplification. The vibration was then measured for different optical pump powers (Fig. 4). For an optical power of $-14\,dBm$ (estimated power at the device) we observe that the apparent mechanical Q (≈10300) has more than doubled compared to the case without feedback (≈4760). When the optical power is increased to $-9\,dBm$ (and $-4\,dBm$) we notice a strong increase of the amplitude and consequently a reduction of the peak linewidth. This regime with regenerative oscillation is sometimes referred to as ṗarametric instability' in the literature [1]. In this regime the peak linewidth of the mechanical oscillation is much smaller than the minimum achievable bandwidth of the electrical spectrum analyzer (10 Hz). In fact the measured peak shape is no longer Lorentzian but rather a convolution of the Lorentzian shape we wish to measure and the Gaussian shape of the electrical band pass filter (from the electrical spectrum analyzer). We found that undoing this convolution in software does not permit a reliable extraction of the linewidth. We can only conclude safely that the linewidth must be much smaller than 10 Hz (so Q≫600000).

In Fig. 5 the results of an experiment for different delay lengths in the feedback loop are

#142630 - $15.00 USD Received 15 Feb 2011; revised 10 Apr 2011; accepted 29 Apr 2011; published 22 Jun 2011

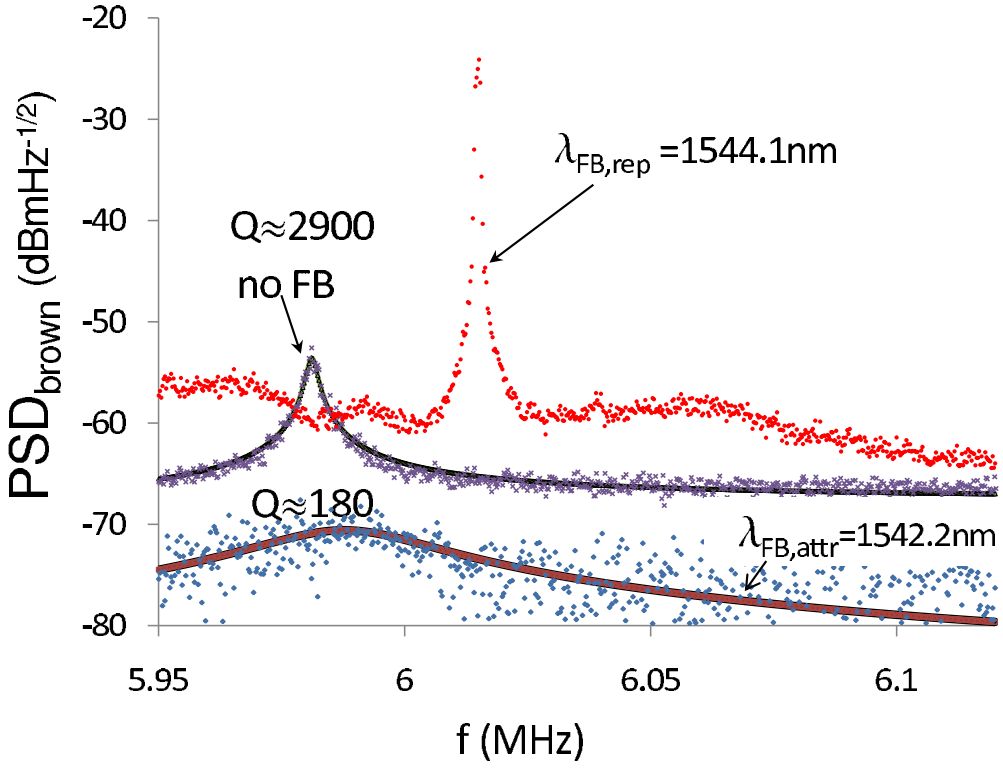

Fig. 6. Pump wavelength tuning allows to switch from the damped regime (curve labeled 'λ_{attr}=1542.2 nm') to the self-pulsating regime (curve labeled 'λ_{rep}=1544.1 nm').

shown. The pump wavelength (λ_{attr}=1542.2 nm for attractive force) and optical pump power are kept constant. (Q≈180, curve labeled '85 ns delay'). The damping is increased over a factor of almost 16 (initial Q=2900). Shortening the feedback loop with 85 ns corresponds approximately to a phase shift of π (mechanical oscillation period ≈168 ns) and consequently strongly amplified motion is found (curve labeled 'negative damping').

Finally we show that in the proposed structure pump wavelength tuning can be used to switch in a flexible way between the damping and amplifying regimes (Fig. 6). Again we set the delay length in order to achieve maximum damping for a purely attractive force (curve labeled '$\lambda_{FB,attr}$=1542.2 nm'). Simply switching the pump wavelength (curve labeled '$\lambda_{FB,rep}$=1544.1 nm') is sufficient to switch between the different regimes.

4. Conclusion

In summary we have obtained wavelength tunable parametric instability of micromechanical oscillators that are fully integrated on a silicon-on-insulator chip. No optical cavity was present in the active optomechanical feedback scheme. In order to push the oscillator operation regime closer to the interesting GHz region future work should focus on increasing the optomechanical interaction. This can most easily be achieved by reducing the gap between the waveguides.

#142630 - $15.00 USD Received 15 Feb 2011; revised 10 Apr 2011; accepted 29 Apr 2011; published 22 Jun 2011